SPE
Society of Petroleum Engineers

SPE 23160

Experimental Study of Gas Rise Velocity and Its Effect on Bottomhole Pressure in a Vertical Well

P. Skalle, U. of Trondheim; A.L. Podio, U. of Texas; and J. Tronvoll, U. of Trondheim
SPE Members

This paper was prepared for presentation at the Offshore Europe Conference held in Aberdeen, 3-6 September 1991.

ABSTRACT

A 500 ft vertical well was used to study slip velocity of air in mud and pressure gradients through a 2.93" annulus (5.43 - 2.50") during continuous two phase flow in flowing liquids and in stagnant liquid columns. The well was instrumented to measure liquid- and air flow rate, surface back pressure and annular pressure gradients.

Tests were undertaken with a broad range of air and liquid rates, different liquid properties, and with the injection of air slugs at different rate combinations. It was possible to detect these slugs as they passed the pressure transducers in the annulus. Results were applied to determine gas rise velocity.

Correlation has been developed for gas rise velocity, which was used to estimate gas and liquid hold up. The in situ gas velocity and terminal settling velocity were determined for both dispersed bubbly flow and slug flow. The resulting pressure gradients have been compared to estimates from 8 different empirical correlations. The best results were obtained by using the Zuber & Findley correlation for holdup estimation with a gas holdup of 0.6 to distinguish the boundary between bubble and slug flow. This high transition value was mainly caused by the geometry of the well (tool joints) and partly by the rheology of the mud. A very good agreement between recorded and estimated downhole pressure was achieved, with a mean error of approximately 1% and a standard derivation of 2.9%.

References and illustrations at end of paper.

INTRODUCTION

During drilling into a shallow gas sand or during circulating out a gas kick it is important to know the bottom hole pressure. If not known, it is difficult to bring the well under control.

Few two-phase studies have been performed in large scale annular geometries. Most have involved tubing with diameters of 2" or less and short distances. The annulus of the experimental model in the present work has a hydraulic diameter of 3", which is equivalent to a 5" OD drill pipe in a 9 5/8" casing or a 8 1/2" hole and has a total length of 550 feet. The drill pipe is mounted with tool joints similar to those in the field.

A problem of experimental two-phase studies is the determination of liquid hold up. Quick operating valves to shut off a representative part of the flowing mixture have been commonly applied, while local capacitance measurements have been used in more recent studies. Hold up was determined in this study through the bubble rise velocity derived from material balance considerations:

$$H_g = \frac{v_g^s}{v_g} \qquad (1)$$

in which v_g^s is the superficial gas velocity (q_g/A), and v_g is the absolute gas bubble velocity in the flowing mixture, which was determined experimentally.

THE PRESSURE GRADIENT EQUATION

Two-phase flow obeys all the basic laws of fluid dynamics. In general, this involves developing expressions for conservation of mass, linear momentum and energy.

As a modification of the general energy equation the one-dimensional pressure gradient in the z-direction may be written

$$\frac{dp}{dz} = \left(\frac{dp}{dz}\right)_g + \left(\frac{dp}{dz}\right)_a + \left(\frac{dp}{dz}\right)_f \quad (2)$$

composed of a gravitational component (g), an accelerational component (a) and a frictional component (f).

The equation is usually adapted for two-phase flow by assuming that the gas-liquid mixture can be considered homogeneous over a finite volume in the pipe.

The gravitational or elevation change component in two-phase flow becomes

$$\left(\frac{dp}{dz}\right)_g = g\,\rho_m \sin\phi \quad (3)$$

where ρ_m is the density of the gas-liquid mixture in the volume under consideration and ϕ the deviation from horizontal. Considering a pipe element which contains liquid and gas, the density of the mixture can be calculated from

$$\rho_m = \rho_L H_L + \rho_g H_g \quad (4)$$

where H_L is the liquid holdup and is defined as

$$H_L = \frac{\text{volume occupied by liquid in the pipe element}}{\text{volume of pipe element}} \quad (5)$$

and

$$H_g = 1 - H_L \quad (6)$$

The experimental determination of H_L has been made in various ways by different investigators.

The acceleration component has been ignored by most investigators, based on various assumptions regarding the relative magnitude of the parameters involved. This is necessary in order to derive a simplified procedure to determine the pressure drop due to change in kinetic energy. In this work the method of Beggs & Brill[1] was applied

$$\left(\frac{dp}{dz}\right)_a = \frac{v_m \cdot v_g^s \cdot \rho_m}{p} \quad (7)$$

where v_m is the mixture velocity $((q_g + q_L)/A)$ and p the pressure at point of interest. The acceleration component was later shown to be negligible for practical purposes.

In horizontal pipe flow the total energy loss is caused by change in kinetic energy and frictional pressure loss only. The frictional pressure loss is caused by viscous shear at the pipe wall. The ratio of wall shear stress, τ_w, to kinetic energy per unit volume, $1/2\ \rho v_m^2$, reflects the relative importance of wall shear stress to total pressure losses. This ratio forms a dimensionless group and defines a friction factor

$$f = \frac{\tau_w}{\rho v_m^2/2} = \frac{2\tau_w}{\rho v_m^2} \quad (8)$$

Transforming shear stress into pressure, the friction gradient in terms of the Moody friction factor, f_m, yields

$$\left(\frac{dp}{dz}\right)_f = \frac{f_m \rho v_m^2}{2d} \quad (9)$$

where d is the pipe diameter.

Two-phase frictional pressure losses must be determined by experiments, and are normally calculated using modified versions of the single phase flow equations. The principal considerations for developing pressure gradient equations, are developing methods for predicting liquid holdup and two-phase friction factor.

Published correlations for vertical flow are normally divided into three categories, as first proposed by Orkiszewski[2]. The differences in theoretical concepts of each category and the corresponding correlations are summarised below.

Category 1

Liquid holdup is not considered in the computation of the mixture density, i.e. no-slip is assumed. Thus, mixture density is based on produced (top-hole) fluids composition, corrected for down-hole temperature and pressure. Only a correlation for two-phase friction factor is required. No distinction is made for different flow regimes. The methods in this category that were studied include:

Poettmann and Carpenter[3]
Baxendell and Thomas[4]
Fancher and Brown[5]

Category 2

Slip, which means relative velocity between the two phases, is considered. The liquid holdup is either correlated separately or combined in some form with the wall friction losses. The friction losses are based on the composite properties of liquid and gas. The same correlation for liquid holdup and friction factor are used for all flow regimes.

Only the Hagedorn and Brown[6] correlation was selected from this category.

Category 3

Both slip and different flow patterns are considered. Thus, methods for determining flow regime transitions are necessary. Once the correct flow regime is established, the appropriate holdup and friction factor correlations are given. These correlations are usually different for each flow regime. Three different correlations from this category have been studied

The Duns and Ros correlation[7]
The Orkiszewski correlation[2]
The Beggs & Brill correlation[1]

THE MODIFIED ANNULAR CORRELATION

Compared to the large amount of research which has been conducted in the area of two phase flow in circular pipes, other geometries have gained little attention. However, developing accurate models for other geometries is necessary. The modified annular flow correlation belongs to category 3 as described above and is based on the basic relationships (eqs. (1) through (9)). The following modifications have been included:

Bubble rise velocity
Pressure loss due to tool joints
Flow regime transition

Rise Velocity

As seen previously, the problem in two-phase flow is to find an appropriate expression for the mixture density, ρ_m, by estimating the liquid holdup, H_L. The liquid holdup or the gas void fraction ($1 - H_L$) depends on the in situ velocity of the gas phase, v_g. The gas velocity is greater than the mixture velocity, v_m, because of the buoyancy effect and the tendency of the gas phase to flow through the central portion of the pipe where local mixture velocity is greater than the average mixture velocity. Both of these effects depend on the existing flow pattern, and various expressions for the gas velocity have been published.

For circular channels in vertical and inclined systems, the in situ velocity of the gas phase has been expressed as the sum of the bubble rise velocity in stagnant liquid, v_t, and the mixture velocity v_m (Zuber and Findley[8] Hasan et al.[9]). Hence

$$v_g = C_0 v_m + v_t \tag{10}$$

C_0 in Eq. 10 is a correction factor resulting from the combined effects of the volumetric flux and gas concentration profiles in the cross-section of the flow channel. The values of C_0 and v_t are defined differently for each flow regime.

For bubble flow and slug flow, experiments[8] have shown that C_0 is about 1.2. Hasan[10] found that the presence of an inner tube did not appear to influence neither the terminal rise velocity, v_t, nor the bubble concentration profile. However, this phenomenon was only tested for a restricted diameter range and has to be further investigated for larger diameters.

For bubble flow, Zuber and Findley calculated the terminal rise velocity from the following expression (in consistent units)

$$v_t = 1.41 \sqrt[4]{\frac{g\sigma(\rho_L - \rho_g)}{\rho_L^2}} \tag{11}$$

in which s is the surface tension. Though the most widely used expression is probably Harmathy's[11] correlation, which is given by

$$v_t = 1.53 \sqrt[4]{\frac{g\sigma(\rho_L - \rho_g)}{\rho_L^2}} \tag{12}$$

For slug flow, Hasan found that the presence of an inner tube tends to make the Taylor bubble nose sharper causing an increase in the terminal rise velocity v_{tT}. Data showed a linear relationship of v_{tT} with the diameter ratio d_i/d_o. Thus, Hasan suggested the following expression for Taylor bubble rise velocity for vertical annular systems

$$v_{tT} = [0.345 + 0.10\,(d_i/d_o)] \sqrt{\frac{g d_o(\rho_L - \rho_g)}{\rho_L}} \tag{13}$$

Pressure Loss due to Tool Joints

When the fluids are circulated through the annulus in the experimental well, the tool joints or collars produce a certain resistance to the flowing fluids. The flow restrictions are shown in Fig. 1. Grupping et al.[12] investigated how collars influenced upward flowing gas slugs. They concluded that major fragmentation occurs when a gas bubble passes a tool joint. They also found that a much stronger fragmentation occurred when the inner tube was concentric, compared to an eccentric inner tube.

This gives reasons to believe that the tool joints will influence the transition from bubble to slug flow. Thus, due to increased turbulence and fragmentation, bubble flow will probably occur at higher gas void fractions than in circular pipes or smooth annuli. Further research is necessary to establish any functional dependencies.

One common way of calculating frictional losses at local features in single-phase flow is to express the resistance of the feature in terms of the equivalent length of straight pipe. In general the equivalent length tends to be somewhat longer for two-phase flows. In single-phase flow the velocity profile is fully developed at a maximum of 10 - 12 pipe diameters downstream of the feature. In two-phase flow this distance is greatly increased (by up to ten times)[13]. Thus, pressure loss due to a sudden contraction or enlargement can be calculated from

$$\Delta p = K_E \frac{1}{2} \rho_m v_m^2 \quad (14)$$

where K_E is a constant depending on the geometry of the feature.

Collier[13] has presented a solution for determination of the less constant for two-phase pressure drop in fittings. The loss constant K_E is composed of two parts

$$K_E = \left[\frac{1}{C_c} - 1\right]^2 + (1 - C_e)^2 \quad (15)$$

where

C_c = contraction coefficient (A_C/A_1)
C_e = enlargement coefficient (A_2)
A_c = area of contraction
A_1, A_2 = area before (1) and after (2) the contraction

K_E in Eq. (15) is obtained from single phase considerations and is assumed to be valid also for two-phase flow. For the experimental well applied in this work K_E determined from the single-phase flow table presented by Collier gives a value of 0.111 for each contraction and 0.121 for each enlargement, thus adding up to 0.232 for each tool joint.

To include effects of restriction-geometry (very sharp edges) and the development of large-turbulence, the loss constant K_E was varied between 0.23 and 0.6 in Eq. (14) during the fitting of estimated pressure gradients to measured ones.

Flow regime transition

Earlier research by Taitel et al.[14] stated that the transition from bubble flow to slug flow occurs at a gas void fraction of about 0.25 when turbulent forces are negligible. At higher flow rates, shear stress caused by turbulence tends to break-up the larger bubbles, inhibiting transition to slug flow when void fraction exceeds the value of 0.25. Taitel et al.[14] showed that even for small gas bubbles, the gas void fraction cannot exceed 0.52. This conclusion was adapted from the fact that tightest packing of uniformly sized bubbles corresponds to a void fraction of 0.52.

Furthermore, it is known that the shape of a moving gas bubble is viscosity dependent. In more viscous fluids the bubbles will assume more streamlined shapes. Increased viscosity also reduces the axial interaction of the bubbles and hence the collision frequency is reduced. Grupping et al.[12] found that in a Kelzan XC polymer solution, when bubbles collided, they did not always coalesce to form larger slugs. It was also observed that the existence of collars and tool joints caused both top and bottom fragmentation of already formed slugs. The transition values above do all refer to a Newtonian liquid phase. However, test results with high-viscous liquids have reported void fractions up to 0.90 in which bubble flow pattern still existed[15].

In addition, the upward velocity of a single bubble varies with its diameter. This implies that different bubble sizes will be distributed randomly in a fluid volume and the theory of equally sized spherical bubbles is not applicable.

These findings support the assumption that the void fraction at which transition to slug flow occurs, is very dependant on viscosity and turbulence. A gas kick in drilling mud (flowing past tool joints) will most likely be on the form "dispersed bubble flow".

EXPERIMENTS

Experimental Set-up

The 550 ft experimental well at the University of Texas at Austin (UT) is permanently completed with a 9 5/8" casing. The well is equipped with two tubings, a 5.90" x 5.43" outer tubing and a 2.5" x 2.0" inner tubing. A standard single wing tree is installed at the top. Eight pressure transducers were installed inside the well at the locations shown in Fig. 2. The pressure transducers wiring was routed through the casinghead valve in special sealing assembly.

Liquid was pumped through a metering station to the well by means of three centrifugal pumps, each with a capacity of 150 gpm. Air was compressed to approximately 300 psig at the surface by two compressors prior to injection. The gas was then sent through a metering unit into the well. The surface equipment is shown in Fig. 3, and includes also a separator and two 500 gal storage tanks.

Gas and liquid were injected through the inner tubing and the outer annulus respectively. The two phases were mixed at the tubing outlet downhole, and flowed to the surface through the inner annulus, as illustrated by the arrows in Fig. 2. Pressure transducer no. 3 was located 180 hydraulic diameters upstream, and this was considered to be a sufficient mixing length. In addition, it was assumed that the gas and liquid phase would distribute homogeneously in the annulus due to the mixing caused by the turbulence at the tool joints.

The returning fluids at the wellhead were conducted to the separator, and the individual phases were separated by gravity. Adjusting the separator pressure made it possible to exert additional pressure to the well (p_{surf}) to simulate various depths.

Significant well and fluid data during the experiments are presented in Table 1. The mud rheology is given in Table 2.

Test Procedure and Data recording

Before starting a series of pressure recordings, the flow situation was stabilised by applying maximum liquid flow rate. The gas rate was then gradually increased to the intended value. The pressure at each transducer in the well was recorded at constant gas rate starting at a high liquid rate which was gradually reduced. The minimum gas rate was limited by the well pressure.

Liquid flow rate was measured by two turbine meters, calibrated by a mass flow meter, to cover both high and low flow rates. The gas flow was recorded by a rotameter for low flow rate measurements while an orifice plate metering row was used for high flow rates. Pressure data from the transducers in the well were recorded in a "DPI 420 multitransducer pressure indicator". All other data were constant for a given test and were thus recorded manually. A typical pressure depth plot is shown in Fig. 4.

RESULTS

Recorded results

The results of the gas velocity measurements and the pressure gradient calculations are presented next.

To determine the empirical constants in Eq. (10); $v_g = C_o\, v_m + v_t$, the in situ velocity of the gas phase, v_g, was plotted against the mixture velocity v_m as shown in fig. 5. v_m was calculated from the sum of recorded input flow rates, while v_g was estimated in the following way: The gas void fraction, H_g, is related to the superficial gas velocity by the material balance consideration

$$H_g = \frac{v_g^s}{v_g} \quad \text{or} \quad v_g = \frac{v_g^s}{H_g} \tag{1}$$

In the experiments the pressure gradient was measured and the void fraction estimated by

$$H_g = 1 - \frac{(dp/dz)_{measured}}{(dp/dz)_{liquid}} \tag{16}$$

Although (dp/dz) measured is dynamic, involving friction and acceleration loss, and $(dp/dz)_{liquid}$ is static and given the value 0.434 psi/ft, this gives a useful estimation of v_g.

The plotted results are shown in Fig. 5 for continuous gas injection, assumed to be dispersed bubble flow.

A new series of tests involved the injection of large slugs of air. It was possible to detect the top of the slugs by means of sharp pressure changes just as they flowed past a pressure trancducer.

Fig. 6 shows the test data for slugs (Taylor bubbles), though v_g is measured at the top of the bubble. The average velocity is thought to be lower.

The dispersed bubble flow and slug flow tests in figs. (5) and (6) were curve fitted. Curve fitting of data from flow test with water and air gave too low data reliability to be presented. The reason for poor results were a) low test range and b) test methodology was not strict enough at those tests. Flow tests with two different mud rheologies gave the following result:

Dispersed bubble flow:

$$\text{Viscosity 1: } v_g = 1.19\, v_m + 0{,}74 \tag{17}$$

$$\text{Viscosity 2: } v_g = 1.19\, v_m + 0{,}99 \tag{18}$$

Slug flow:

$$\text{Viscosity 1: } v_g = 1.25\, v_m + 2.45 \tag{19}$$

$$\text{Viscosity 2: } v_g = 1.15\, v_m + 2.45 \tag{20}$$

The resulting values of C_o. are in average equal to 1.2, both for dispersed bubble flow and for slug flow. This is in very good agreement with previsous presented results on C_o[9,10,15].

The terminal rise velocity, v_t, is equal to 0,74 and 0,99 ft/s for viscosity 1 and 2 respectively in dispersed bubble flow, and 2,45 ft/s for both muds in the slug flow regime.

The bubble rise velocities were also calculated by using Eqs. (11-13). For the bubble flow regime, Eq. (11) gives approximately

$$v_t = 1.41\sqrt[4]{0.0981 \cdot 65.0/10^4} \cdot 3.281 = 0.735 \text{ ft/sec}$$

and Eq. (12) gives approximately

$$v_t = 1.53\sqrt[4]{0.0981 \cdot 65.0/10^4} \cdot 3.281 = 0.797 \text{ ft/sec}$$

Thus, according to these values and the result obtained from Fig. 5 (Eqs. (17) and (18)), a terminal rise velocity of 0.75 ft/s was selected for later applications.

For slug flow regime, Eq. (13) yields an approximate value of

$$v_{tT} = [0.345 + 0.10\,(2.50/5.43)]\sqrt{32.2 \cdot 5.43/12} = 1.49 \text{ ft/sec}$$

and this value was applied as terminal slug rise velocity. From Fig. 6 (Eqs. (19) and (20)) it can be seen that the top of the bubble has a higher velocity than 1.49 ft/sec.

It was also investigated if the size of the slug could influence on the terminal travel time. In one of the experiments the gas injection volume was gradually increased, and the resulting slug velocity is presented in fig. 7. From this figure it can be seen that the top bubble travel time is varying between 1.5 ft/s for small slugs and 2.5 ft/s for large slugs. The capacity of the flow loop seems to be reached at a bubble size of 110 scft.

Calculated pressure gradients

From all the pressure data points that were gathered, the measured bottom hole pressure was compared to the calculated bottomhole pressure. Pressure gradients were calculated in accordance with 8 of the previously discussed correlations in addition to the modified correlation. In the modified correlation three modifications are included; a) the influence of higher pressure losses due to tool joints, b) the influence of later flow regime transition and c) the hold up calculation is based on the exact estimation of bubble rise velocity. To obtain a measure of the accuracy of the investigated correlations a statistical analysis was performed. The results are given in table 3.

It should be mentioned that the observed pressure is recorded by pressure-transducer no. 1 (see Fig. 2). Thus, the experimental well had a simulated depth of 504.64 ft, and the calculated bottom hole pressure is the actual pressure at this location. The surface pressure is obtained by transducer no. 8, which is mounted at the annulus exit.

Results for four correlations, one from each category, are presented graphically in Fig. 8. All calculated pressures are lower than recorded pressure.

The modified correlation had several parameters which could be individually adjusted.

However, all parameter values were based on published expressions and own results.

Through a methodic variation of the transition value it was found that the transition from bubble flow to slug flow regime that best fitted calculated pressure to observed bottom hole pressure at a gas void fraction of 0.60 for the viscosities used in the experiments.

DISCUSSION

The gas supply at the well bottom was varying due to fluctuations in the compressor pressure. The resulting fluctuating in the average gas flow rate was, nevertheless, negligible.

Liquid flow rate has been checked by a mass flow meter. The calibration showed a rate dependent error, which revealed that the obtained volume flow-meter rates used for comparison could involve errors up to 2.5%.

The measuring instruments do not involve any considerable inaccuracies. The pressure transducers have an error of ± 1% of full scale.

General observations

The different correlations tested seem to have some features in common. The only exception is the Beggs and Brill method which is based upon flow pattern transitions for horizontal pipes.

All the correlations seem to underestimate the bottom hole pressure to a various extent. A proper explanation of this behaviour is difficult to find. Magcobar Mud Manual[16] proposes that the viscoelastic effects of polymer fluids are important in sudden changes of cross sectional area such as tool joints and collars. The rapid change in deformation to which the fluid is subjected causes an increase in the pressure gradient. This effect is not included in any of the original correlations and might thus be one of the reasons for the higher measured than predicted pressure.

Another common behaviour is the fact that most of the correlations show a clear tendency to improve their accuracy with increasing bottom hole pressure, is interesting. This can also be seen by the severe scatter of data points at low liquid and gas rates in Fig. 9. The estimated data are obtained by using the Duns and Ros correlation.

The discrepancy in the terminal rise velocities obtained from Fig. 6 is assumed to be mainly caused by considerable scatter in the rheological data of viscosity group 2. The slightly higher viscosity in these data also caused an increased bubble rise velocity also as proposed by Grupping et al.[13].

Frictional pressure drop

Calculated frictional pressure drop based on three common rheological models resulted in considerable discrepancies between the three. As can be seen from Fig. 10, the Dodge and Metzner method gave surprisingly a frictional pressure loss up to twice as high as the Bingham friction loss.

It is assumed that one reason for these differences, is the encountered range of the flow behaviour index n due to the fact that the frictional pressure drop is dependent on the flow behaviour index n. This has been revealed by experiments of Jensen and Sharma[18]. A common flow behaviour index range for mud is between 0.5 and 1.0 while the flow behaviour index in the polymer mud of this work are within 0.35 and 0.53 as displayed in Table 2.

Future studies

The two killing methods called Bull heading and Volumetric Method have up to now not been extensively studied on experimental basis. The laboratory equipment at the University of Texas at Austin is well suited for such studies. Available computer programs for two-phase downward flow are now being tested and fitted for this purpose.

CONCLUSIONS

Full scale investigations of two-phase flow, through geometry and with fluid rheologies typical for shallow drilling operations have been carried out. The results are confirming earlier investigations, even though previous investigations mostly have been performed in small diameter pipes and with Newtonian fluids.

For dispersed bubble flow the in situ gas velocity can be estimated (in ft/sec.) through the empirical relationship

$$v_g = 1{,}2\, v_m + 0{,}75$$

The in situ velocity of a gas slug can be estimated through the equation

$$v_g = 1{,}2\, v_m + 1{,}5$$

The terminal velocity of 1.5 ft/sec was only partly confirmed since the experimental set up was only capable of recording the movement of the top interface of the gas slug.

As a result of the presented study, the following conclusions can be drawn:

- Drilling underbalanced through a gas reservoir will result in a two-phase mixture of drilling mud and formation gas which have to be considered. During normal kick conditions only the dispersed bubble flow pattern will probably occur. This is due to a transition boundary between bubble and slug flow given by a gas void fraction of 0.6 (for the experimental configuration). This high transition void fraction is caused by the turbulent forces exerted by the tool joints which fragment the larger bubbles. The viscosity of the drilling mud is also assumed to increase this transition value.

- The simplified correlations of category 1 (no-slip assumed and liquid holdup not considered) were found to be inadequate for the flow conditions encountered while drilling. The Hagedorn and Brown correlation (from category 2) which usually gives good over-all prediction results, was also found to be inaccurate. This was caused by the late transition from bubble flow behaviour to slug flow.

- Over the range of parameters covered by the data, the best results were obtained by using the Zuber and Findlay correlation for holdup estimation and the modified criteria to distinguish between bubble and slug flow. A very good agreement have been achieved with a standard deviation of 2.9%.

- The Duns and Ros method was found to be the second most accurate correlation. The bottom hole pressures were underestimated with an mean error of -3.7% and a standard deviation of 2.8%.

- The frictional component does not contribute more than maximum 5 percent to the total pressure gradient. The accelerational component is negligible.

- Tool joints and collars exert a significant contribution to the frictional pressure loss. However, further research on the extension of single phase theory to two-phase conditions, and also on the identification of the

functional dependency of the transition void fraction on viscosity, tool joints and other parameters are necessary.

NOMENCLATURE

A = cross sectional area
C_o = velocity profile factor
d = diameter
f = friction factor
g = gravitational constant
H = hold up or void fraction
K_E = geometry dependent energy loss constant
p = pressure
q = volumetric flow rate
t = time
v = velocity
v^s = superficial velocity
z = vertical coordinate

Greek

ε = surface roughness
μ = viscosity
ρ = density
τ = shear stress
ϕ = porosity
σ = surface tension

Subscripts

a = acceleration
f = frictional
g = gas or gravitational
i = inner (diameter)
L = liquid
m = mixture (of water and gas)
o = outer (diameter)
t = terminal
T = Taylor
w = wall

REFERENCES

1. Beggs, H.D. and Brill, J.P.: "A Study of Two-Phase Flow in Inclined Pipes", J. Pet. Tech., May 1973; 607-617, Trans AIME, 255.

2. Orkiszewski, J.: "Predicting Two-Phase Pressure Drops in Vertical Pipes", J. Pet. Tech., June 1967; 829-838.

3. Poettmann, F.H. and Carpenter, P.G.: "The Multiphase Flow of Gas, Oil and Water Through Vertical Flow Strings with Application to the Design of Gas-Lift Installations", Drill. and Prod. Prac., API 1952; 257-317.

4. Baxendell, P.B. and Thomas, R.: "The Calculation of Pressure Gradients in High-Rate Flowing Wells", J. Pet. Tech., May 1973; 607-617.

5. Fancher, G.H. jr. and Brown, K.E.: "Prediction of Pressure Gradients for Multiphase flow in Tubing", Soc. Pet. Eng. J., March 1963; 59-69

6. Hagedorn, A.R. and Brown, K.E.: "Experimental Study of Pressure Gradients Occurring During Continuous Two-Phase Flow in Small-Diameter Vertical Conduits", J. of Pet. Tech., April 1965; 475-484.

7. Duns, H. Jr. and Ros, N.C.J.: "Vertical Flow of Gas and Liquid Mixtures in Wells", 6th World Pet. Congress Proc., 1963; 451-465.

8. Zuber, N. and Findley, J.A.: "Average Volumetric Concentration in Two-Phase Flow Systems", J. Heat Transfer 87; 453-468.

9. Hasan, A.R. and Kabir, C.S.: "Predicting Liquid Gradient in A Pumping Well Annulus", SPE Prod. Eng., Feb. 1987.

10. Hasan, A.R.: "Two-Phase Up-Flow in Vertical and Inclined Annuli", University of North Dakota, 1989.

11. Harmathy, T.Z.: "Velocity of Large Drops and Bubbles in Media of Infinite or Restricted Extent", AlChE J. t, 1960; 281.

12. Grupping, A.W., Hofland, J.P. and Hermsen, F.J.: "Major fragmentation of gas slugs caused by collars", Oil & Gas Journal, Dec. 1986; 105-110.

13. Collier, J.G.: "Convecting Boiling and Condensation", McGraw-Hill Book Co. Inc., New York City, 1981.

14. Taitel, Y., Bornea, D. and Dukler, A.E.: "Modelling Flow Pattern Transitions For Steady Upward Gas-Liquid Flow in Vertical Tubes", AlChE J., May 1980; 345-354.

15. Govier, G.W. and Aziz, K.: "The Flow of Complex Mixtures in Pipes", Van Nostrand Reinhold, New York City, 1972.

16. Magcobar - Division Oilfield Products Group: "Drilling Fluid Engineering Manual, Dresser Industries Inc., Houston, Tx.

17. Dodge, D.G. and Metzner, A.B.: "Turbulent Flow of Non-Newtonian Systems", AlChE J. 5, 1959; 189.

18. Jensen, T. and Sharma, M.P.: "Analysis of Friction Factor and Equivalent Diameter Correlations for Annular Flow of Drilling Fluids", 10th Annu. ASME Energy-sources tech. conf., Drilling Symp. Proc., Dallas, Feb. 1987.

Fig. 1 Geometry of the flow restrictions (tool joints) in the experimental well.

Fig. 2 Sketch showing the fluid flow path and the pressure metering stations no. 1 to 8 in the UT experimental well. The vertical distances are given in feet.

Fig. 3 Schematic layout of fluid and gas flow system and surface operational and control equipment.

Fig. 4 A typical pressure-depth plot for one of the two-phase flow tests.

Fig. 5 Gas velocity for dispersed bubble flow in water, mud 1 and mud 2.

Fig. 6 Gas velocity for slug flow (Taylor bubble) in water, mud 1 and mud 2.

Fig. 7 Stagnant gas slug velocity vs. injected bubble volume. Velocity were calculated from travel time of slug top from bottom of well to pressure transducer no. 4, 5 and 7.

Fig. 8 Predicted bottom pressure vs. measured pressure from four selected correlations; Poettmann & Carpenter (Category 1), Hagedorn & Brown (Category 2), Beggs & Brill (Category 3) and Modified correlation (Category 3).

Fig. 9 Error in bottomhole pressure prediction applying the Duns & Ros correlation. The average error is a function of liquid and gas flow rate.

Fig. 10 Predicted frictional pressure drop using different models as a function of liquid flow rate and gas flow rate.

Table 1 Significant well and fluid data in the experiment.

Table 2 The rheology of the water based mud (Kelzan XC) throughout the tests. The average rheology of "viscosity 1-mud" and "viscosity 2-mud" were: PV_1 = 2 cP, YP_1 = 3 lb/100 ft^2 PV_2 = 3 cP, YP_2 = 5,5 lb/100 ft^2

Table 3 Overall results from the ivestigated correlations. Calculated bottom hole pressures are compared with recorded.

TABLE 1—SIGNIFICANT WELL AND FLUID DATA IN THE EXPERIMENT

Well Data	Oilfield Units (OU)	SI Units
D_{well}	550 ft	167.9 m
D_{tub_i}	d_o : 2.50" d_i x 2.00"	d_o : 63.5 mm d_i x 50.8 mm
D_{tub_o}	d_o : 5.90" d_i x 5.43"	d_o : 149.9 mm d_i x 137.9 mm
p_{surf}	32.2 - 73.9 psia	2.22 - 5.10 · 10^5 Pa
T_{surf}	75.0° F/ft	24.0° C
$\Delta T/\Delta z$	0.0° F/ft	0.0° C/m
ε/d	0.0006	0.0006
Numb. of tooljoints	17	17
Fluid Data		
q_L	0 - 128 gpm	0 - 8.074 · 10^{-3} m^3/s
$q_{g_{surf}}$	0 - 10818 scft/h	0 - 0.0851 m^3/s
ρ_L	62.4 lb/ft^3	1000 kg/m^3
$\rho_{air_{stc}}$	0.0625 lb/ft^3	1.23 kg/m^3
μ_g	0.02 cP	2.0 · 10^{-5} Pas
$\sigma_{air\text{-}mud}$	65.0 dyn/cm	0.065 N/m

TABLE 2—THE RHEOLOGY OF THE WATER-BASED MUD (KELZAN XC) THROUGHOUT THE TESTS
The average rheologies of "viscosity 1-mud" and "viscosity 2-mud" were: $PV_1 = 2$ cP, $YP_1 = 3$ lb/100 ft^2, $PV_2 = 3$ cP, $YP_2 = 5.5$ lb/100 ft^2.

DATE	TIME	FLUID	SHEAR STRESS (LBS/100 ft^2) AT RPM:			
			600	300	200	100
26.02.89		water				
27.02.89		water				
28.02.89	10:50	visc 1	9	6,5	6	4
	13:10	visc 1	8,5	6	5	3,5
01.03.89	8:00	visc 1	7,5	5,5	4,5	3,5
	8:35	visc 1	7,5	5,5	4,5	3,5
	9:30	visc 1	7,5	5,5	4,5	3,5
	14:27	visc 1	7,25	5,5	4,5	3,5
	15:07	visc 1	7	5	4,25	3,25
	15:55	visc 1	7	5	4,25	3,25
	18:12	visc 1	7	5	4	3,25
02.03.89	10:55	visc 1	7	5	4	3
	14:30	visc 1	6,5	4,75	4	3
03.03.89	9:45	visc 1	7,5	5,5	4,5	3,25
	10:15	visc 1	7,5	5,5	4,5	3,25
	14:15	visc 1	7	5	4	3
		visc 1	6,5	4,5	3,75	2,75
		visc 1	6,5	4,5	4	3
06.03.89	9:00	visc 2	11,5	8,5	7,5	5,5
	10:00	visc 2	11,5	8,5	7,5	5,75
	10:30	visc 2	11,25	8,5	7,25	5,5
	10:45	visc 2	11,25	8,5	7,25	5,75
	11:00	visc 2	11,25	8,75	7,5	5,75
	19:00	visc 2	11,5	8,75	7,5	6
	20:00	visc 2	11,5	8,5	7,25	5,5
	21:00	visc 2	11	8,25	7,25	5,5
07.03.89	9:30	visc 2	10,75	8,25	7	5,5
	14:25	visc 2	10,5	8,25	7,25	5,25
08.03.89	15:00	visc 2	10,25	7,5	6,5	5
	16:00	visc 2	10	7,25	6	4,5
	17:00	visc 2	10	7	6	4
	18:00	visc 2	9,25	6,5	5,5	4
09.03.89	9:00	visc 2	10,25	7,5	6,5	4,5
	10:00	visc 2	10	7,25	6	4

TABLE 3—OVERALL RESULTS FROM THE INVESTIGATED CORRELATIONS. CALCULATED BOTTOMHOLE PRESSURES ARE COMPARED WITH RECORDED.

Prediction method	Viscosity 1		Viscosity 2	
	Av. %-error	% St. dev.	Av. %-error	% St. dev.
Poettmann & Carpenter	-26.73	14.36	-22.90	16.77
Baxendell & Thomas	-26.72	14.37	-22.89	16.78
Fancher & Brown	-30.30	18.04	-29.24	19.16
Hagedorn & Brown	-37.13	11.06	-36.92	12.22
Duns & Ros	-3.68	2.82	-5.48	4.50
Orkiszewski	-18.53	10.65	-20.08	11.96
Beggs & Brill	-3.36	8.26	-5.29	6.30
Modified correlation	0.01	2.92	-1.19	5.26

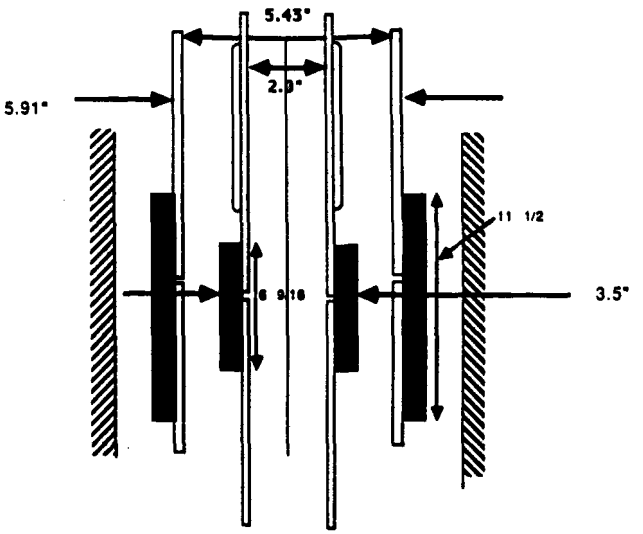

Fig. 1—Geometry of the flow restrictions (tool joints) in the experimental well.

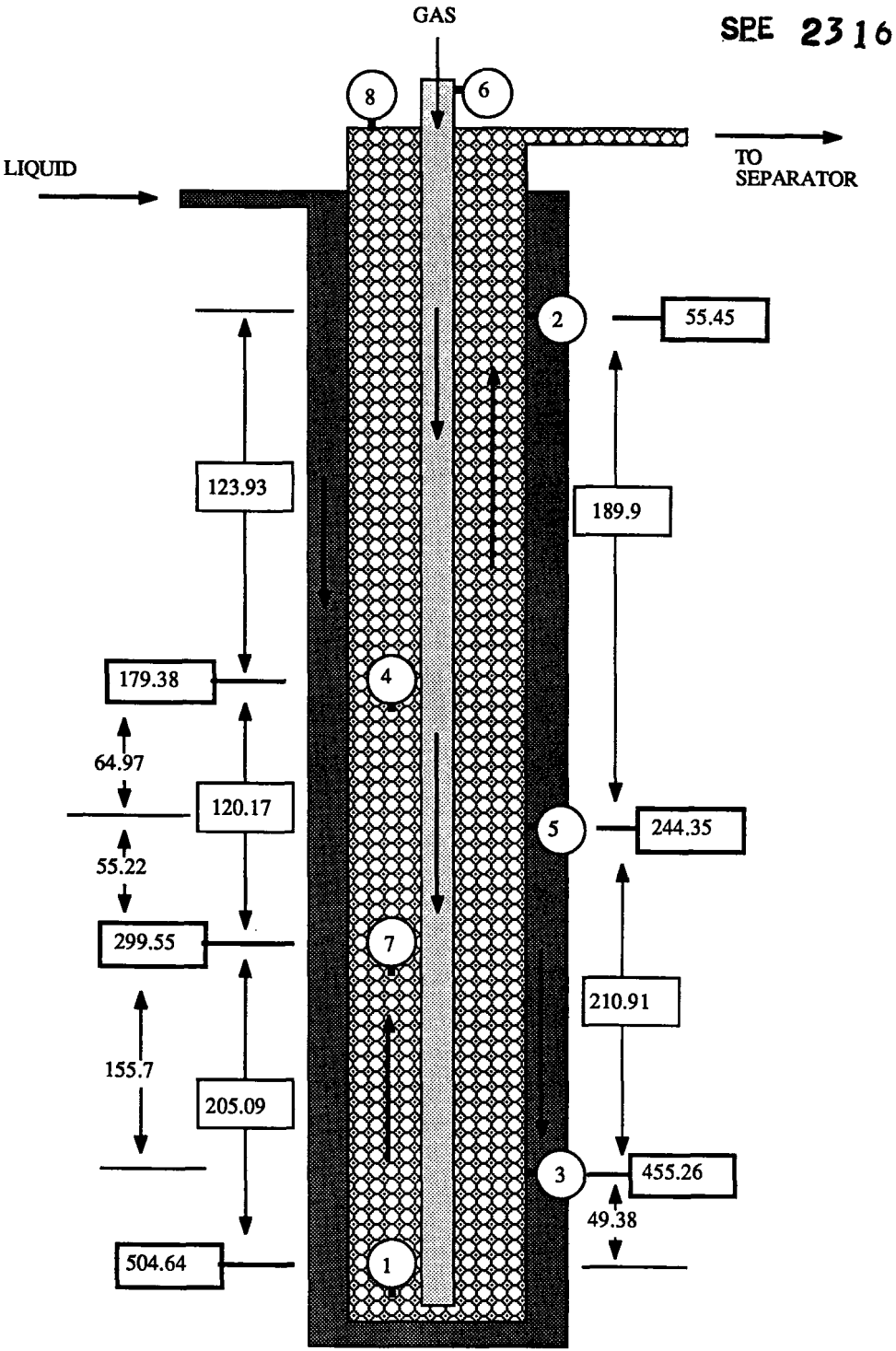

Fig. 2—Sketch showing the fluid-flow path and the pressure metering stations Nos. 1 to 8 in the UT experimental well. The vertical distances are given in feet.

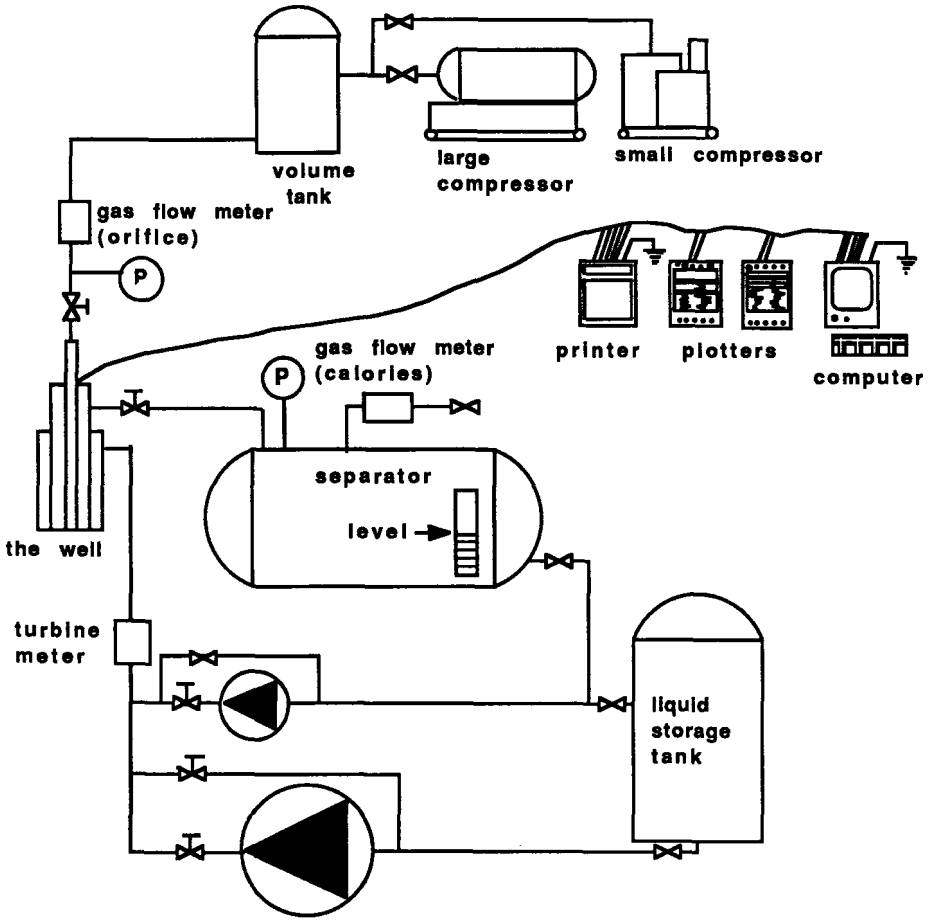

Fig. 3—Schematic layout of fluid and gas flow system and surface operational and control equipment.

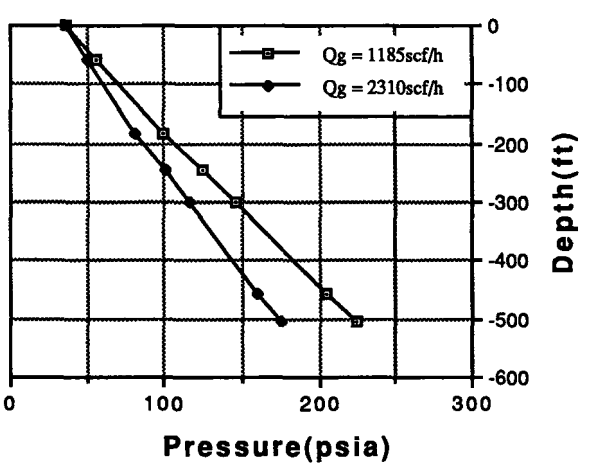

Fig. 4—A typical pressure-depth plot for one of the two-phase flow tests.

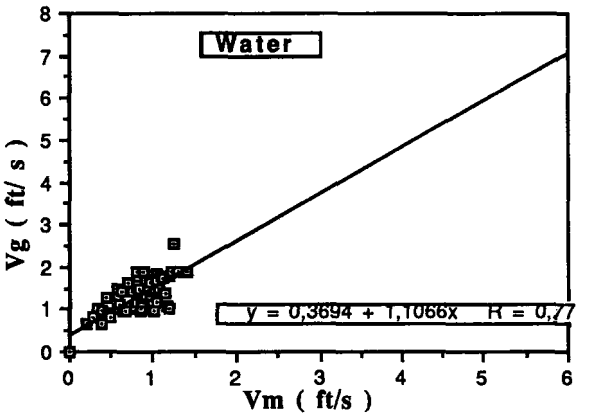

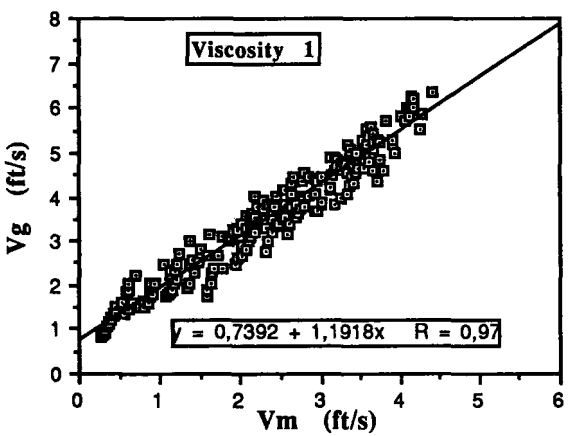

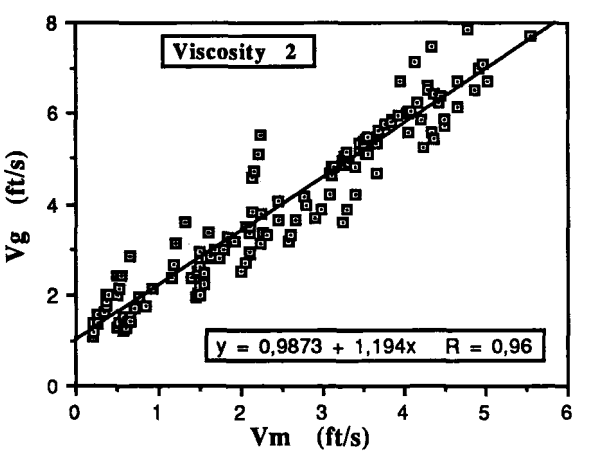

Fig. 5—Gas velocity for dispersed bubble flow in water, Muds 1 and 2.

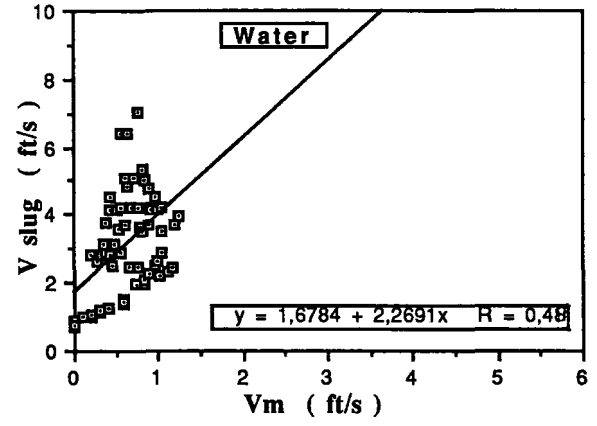

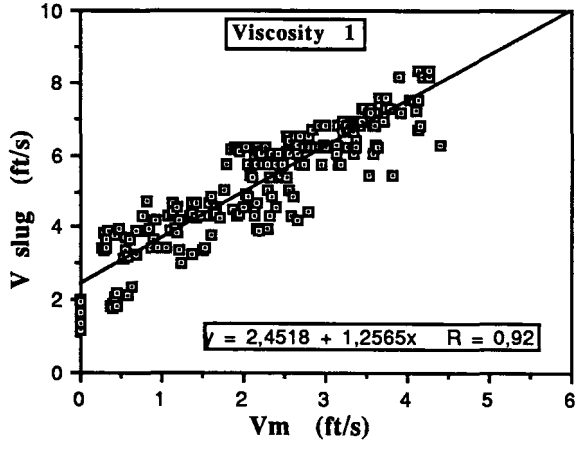

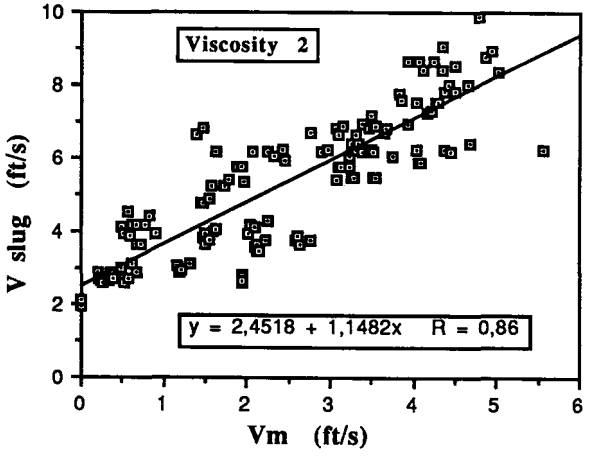

Fig. 6—Gas velocity for slug flow (Taylor bubble) in water, Muds 1 and 2.

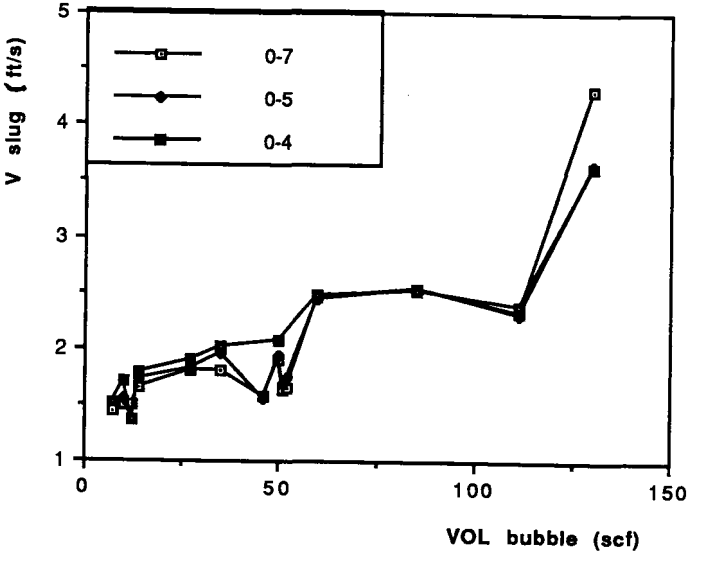

Fig. 7—Stagnant gas slug velocity vs. injected bubble volume. Velocity was calculated from travel time of slug top from bottom of well to pressure transducers Nos. 4, 5, and 7.

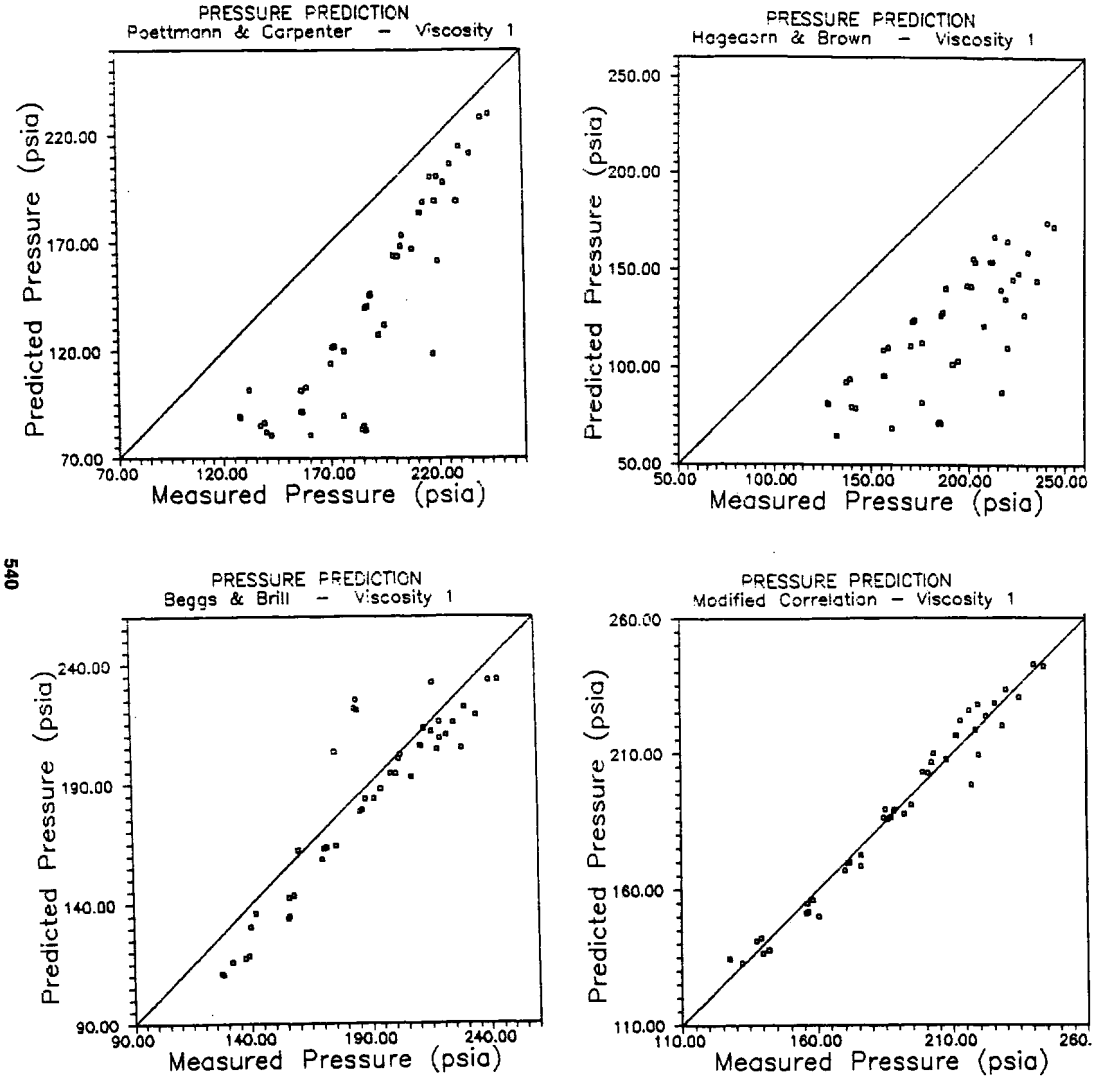

Fig. 8—Predicted bottom pressure vs. measured pressure from four selected correlations: Poettman and Carpenter (Category 1), Hagedorn and Brown (Category 2), Beggs and Brill (Category 3), and modified correlation (Category 3).

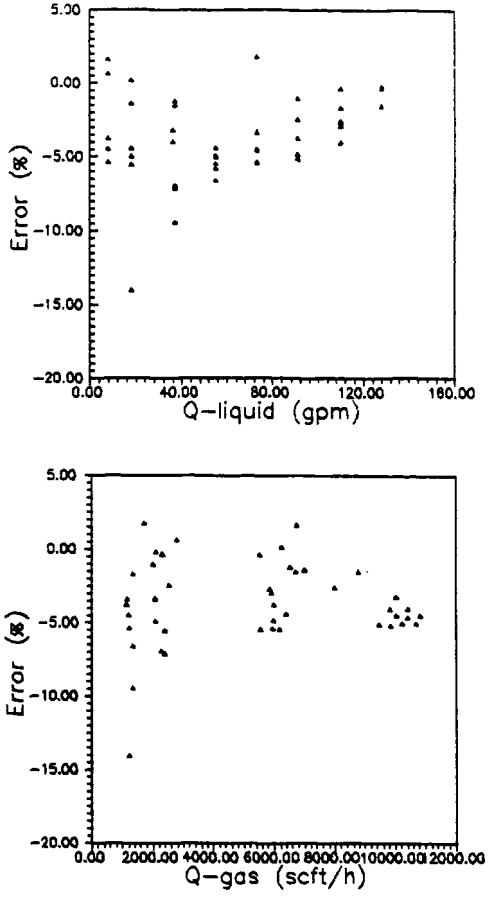

Fig. 9—Error in bottomhole pressure prediction applying the Duns and Ros correlation. The average error is a function of liquid and gas flow rates.

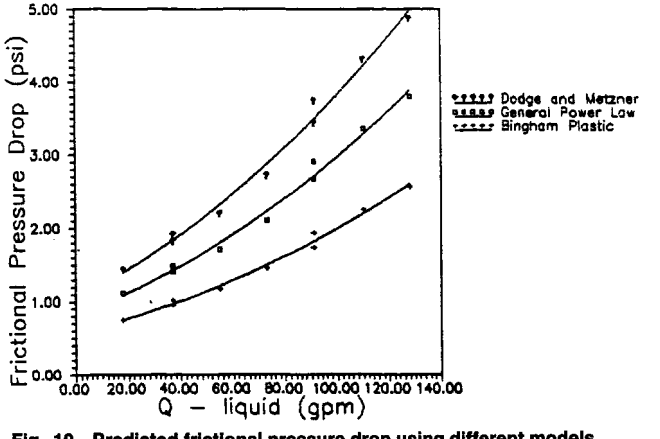

Fig. 10—Predicted frictional pressure drop using different models as a function of liquid flow rate and gas flow rate.